ELSEVIER

Journal of Photochemistry and Photobiology A: Chemistry 124 (1999) 147–152

Journal of Photochemistry and Photobiology A:Chemistry

Self-organized *J* aggregates of pseudoisocyanine dye in nanometer dimensions at the vicinity of a glass/solution interface: a time-resolved and total-internal-reflection fluorescence spectroscopic study

Hiroshi Yao*, Hiroshi Ikeda, Ren Kawabata, Noboru Kitamura[1]

Division of Chemistry, Graduate School of Science, Hokkaido University, Kita-ku, Sapporo 060-0810, Japan

Received 12 February 1999; received in revised form 29 March 1999; accepted 6 April 1999

Abstract

Optical properties of newly observed *J* aggregates (J_{L1} and J_{L2}) for an aqueous pseudoisocyanine (PIC) dye solution produced in a soda lime wedge-type glass cell at room temperature were demonstrated. The absorption peaks of the aggregates were red-shifted (peak: J_{L1}∼17 340 and J_{L2}∼17 240 cm^{-1}) compared to that of a well-known *J* aggregate (peak: ∼17 480 cm^{-1}), and their line widths were also broadened. Time-resolve and total-internal-reflection (TIR) fluorescence measurements showed that the *J* aggregates were distributed in a mesoscopic region at the glass/solution interface, and the aggregate/substrate interface in solution could act as a nonradiative channel for the excitonic state.

Keywords: *J* aggregate; Pseudoisocyanine; Interface; Time-resolved fluorescence spectroscopy; Total-internal-reflection fluorescence

1. Introduction

Molecular aggregates play important roles in various fields of science and are often found in biological systems, where transport of a photon energy and an electron takes place very efficiently [1]. Organic dye aggregates have been also utilized for technological applications: photography and opto-electronics [2]. Among various organic dyes, cyanine dyes represented by pseudoisocyanine (PIC) produce so-called *J* aggregates, as characterized by red-shifted (with respect to the monomer band energy), intense, and very narrow excitonic absorption (*J* band). Recently, *J* aggregates have attracted considerable attention in relation to molecular assemblies or coherent excitation phenomena which provide large optical nonlinearities [3–7]. As the molecular structure of the *J* aggregate, a linear chain structure has been proposed. Knapp has shown that the spectral line profile is related to the number of coherently coupled molecules (N_c) in the aggregate and should become narrow by a factor of $N_c^{1/2}$ as compared to that of the monomer spectrum [8]. More precisely, the correlation between molecular transition energies of neighboring molecules within the aggregate affects the line shape of the *J* band through a disorder parameter *D* [9]. In spite of such extensive studies, however, the definite structure and aggregation number of the *J* aggregate of PIC have been a matter of controversial discussions.

A study on optical dynamics of the *J* aggregates is also of primary importance since the study provides information about coherent excitation. Molecules within a coherence size (N_c) of the aggregate respond in phase to an external field and, as a result, the radiative decay rate is predicted to increase by a factor of N_c. Theoretical calculations have shown that the coherence size is dependent on a coupling strength between the molecules and a temperature [7]. Actually, it has been elucidated that exciton–exciton annihilation often dominates excited state relaxation of the aggregates [10,11], and the fluorescence lifetime of the PIC *J* aggregates in water has been determined to be several hundreds of picosecond at room temperature under a low power excitation condition [12]. Superradiance of the PIC *J* aggregate has been reported on the basis of detailed temperature-dependent lifetime studies in a water/ethylene glycol glass: 40 ps below 50 K while it increases with increasing temperature [13]. The lifetime of the PIC *J* aggregates in LB monolayer films was also determined to be 8.2 ps at room temperature [14]. In the case of a thiacarbocyanine *J* aggregate adsorbed on AgBr microcrystals, a

*Corresponding author.

[1]Co-corresponding author.

1010-6030/99/$ – see front matter
PII: S1010-6030(99)00083-0

very short lifetime with ca. 5–25 ps was observed at room temperature.

Optical properties of the *J* aggregates have been examined extensively for solution, LB film, and adsorbed states as described above and those are shown to be sensitive to microenvironments. Clearly, ordered structures in LB and on adsorption sites of crystal surfaces are favorable factors for producing molecular arrangements. On the other hand, glasses are an amorphous material and its effect on an ordered molecular aggregation similar to that on crystal surfaces is not expected. Thus, optical measurements have been performed generally by using glass cells. In the course of studying spectroscopic characteristics of aqueous PIC solutions in minute dimension, however, we found for the first time several types of surface-induced, self-organized *J* aggregate formation of PIC at a soda lime glass/water interface. Since the observed *J* aggregate exhibited an absorption peak and a line width different from those of a well-known *J* aggregate of PIC (peak: $\sim$17 480 cm^{-1}, width: $\sim$70 cm^{-1} (HWHM) at room temperature) [15], we explored detailed spectroscopic measurements on the newly observed *J* aggregates including time-resolved and total-internal-reflection (TIR) fluorescence spectroscopies. In this article, we report characteristic features of the optical and morphological properties of the self-organized *J* aggregates produced at a glass/water interface.

2. Experimental

1,1′-Diethyl-2,2′-cyanine (pseudoisocyanine; PIC) chloride was obtained from Nippon Kankoh-Shikiso Kenkyusho and used as received. Pure water was obtained by an Aquarius GSR-200 (Advantec). Soda lime glass, borosilicate glass (Matsunami Glass Industries), and quartz glass plates (Fujiwara) were used to prepare wedge-type optical thin-layer cells. Major components of the soda lime glass used were SiO_2 (70%), Na_2O (12%), CaO (6.5%), and K_2O (4%). A borosilicate glass used was mainly composed of SiO_2 (65%), B_2O_3 (10%), and K_2O (8%). The optical path length of the thicker side of the wedge cell was set about $\sim$30 μm by using an aluminum spacer, while no spacer was set in the other side. An aqueous PIC solution (6 mM) as a sample was introduced to the cell by capillary action from the thicker side. The total length of the cell was 25 mm.

Absorption spectra were measured with a Hitachi U-3300 spectrophotometer. Fluorescence spectra were obtained using a Hitachi F-4500 spectrofluorometer or polychromator-multichannel photodetector set (PMA-11, Hamamatsu Photonics). Fluorescence quantum yields of the *J* aggregates were determined by observing the fluorescence from the cell front with rhodamine 101 in ethanol being used as a standard (quantum yield=0.98 [16,17] at 560 nm excitation). Fluorescence lifetimes were determined by a time-correlated single photon counting system (Hamamatsu Photonics, SPC-300). Regeneratively amplified (Coherent, RegA 9000) output pulses of a solid-state green laser (Coherent, Verdi) pumped mode-locked Ti:saphirre laser (Coherent, Mira 900 F) were introduced to an optical parametric amplifier (Coherent, OPA 9400) to obtain excitation pulses at 514 or 570 nm (duration: $\sim$150 fs, repetition: 100 kHz). Emission from a sample was detected with a monochromator (Jobin–Yvon, H-20 UV)-MCP photomultiplier (Hamamatsu Photonics, C2773) set.

Total-internal-reflection (TIR) fluorescence spectroscopy was performed by a system reported earlier [18,19]. Briefly, a sample cell composed of a fused silica hemicylindrical prism/matching oil/thin optical cell was firmly mounted on a rotating stage. The refractive indices of the hemicylindrical prism, the matching oil, the soda lime glass and the aqueous solution are 1.458, 1.475, 1.52 and 1.33, respectively [18]. A 514.5 nm beam from an Ar^+ laser (Coherent, Innova 70, $\sim$1 mW) polarized perpendicularly with respect to the reflection plane was passed through a pinhole (400 μm) and used for excitation. The beam at an incident angle of θ_i was impinged to the glass/solution interface. Fluorescence from a sample was detected at an angle θ_o (observation angle) with a polychromator-multichannel photodetector set (PMA-11). The performance and reliability of the present system were checked by using an aqueous rhodamine B solution (0.3 mM) as a standard sample [18,19].

A TIR fluorescence intensity, I_f, is given by [19]

$$I_f = k|F(\theta_i)|^2|F(\theta_o)|^2 \int_0^L C(z) \cdot \exp\left(-\frac{2z}{d_p}\right) dz, \quad (1)$$

where k is a proportional factor, and $F(\theta_i)$ or $F(\theta_o)$ is the Fresnel factor for θ_i or θ_o, respectively. L is the thickness of a sample, and $C(z)$ is a fluorescent probe concentration at a distance z from the interface. d_p represents a penetration depth of incident light and is a function of the wavelength of incident light (λ), refractive indices of the glass (n_1) and solution (n_2), and absorption index of a sample (κ) [19]. The Fresnel factors are expressed as a function of n_1, n_2, θ_i, and κ [20]. The I_f value is expressed by Laplace transformation of the concentration distribution of a probe in a sample as in Eq. (1)[20]. In the present study, we assume that $C(z)$ is expressed as an exponential profile as in Eq. (2)

$$C = C_0 \exp\left(-\frac{z}{h}\right), \quad (2)$$

where h is a probe distribution parameter. A depth profile for a probe concentration can be thus calculated from Eqs. (1) and (2) with h and κ as parameters.

3. Results and discussion

3.1. Absorption spectroscopy

Fig. 1 shows absorption spectra of an aqueous PIC solution (6 mM) at room temperature determined at the positions

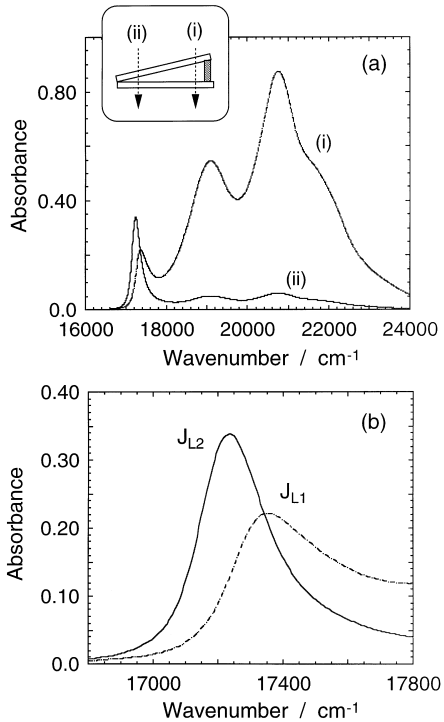

Fig. 1. Absorption spectra of an aqueous PIC solution (6 mM) in a wedge soda lime glass cell. (i) and (ii) show the cell positions for the measurements. The spectra shown in (b) are those at around the *J* bands observed in this study.

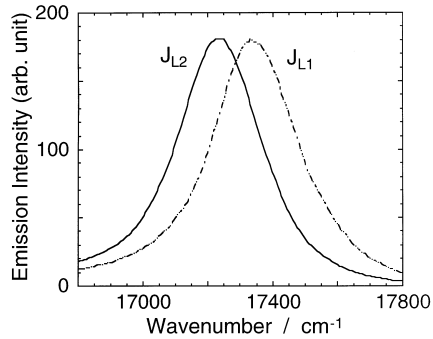

Fig. 2. Fluorescence spectra of the J_{L1} and J_{L2} aggregates.

of (i) and (ii) in a wedge cell as illustrated in the inset of the figure. The optical path length at (i) or (ii) was about 30 or 1.5 μm, respectively, and the distance between two positions was about 25 mm. Beside the monomer (19 200 cm^{-1}) and dimer bands (20 800 cm^{-1}), a new absorption band ascribed to self-organized *J* aggregates was observed at around 17 300 cm^{-1}. However, the band position determined at (ii) was red-shifted compared to that observed at (i) as clearly seen in Fig. 1(b). For simplicity, we attribute the high (17 340 cm^{-1}) and low energy *J* bands (17 240 cm^{-1}) as J_{L1} and J_{L2}, respectively. In addition to the band position, the spectral line width ($\Delta\nu$) of J_{L2} (110 cm^{-1}; HWHM) was narrower than that of J_{L1} (130 cm^{-1}).

The absorption spectrum of the J_{L1} aggregate was similar to that reported for stearic acid/PIC bromide LB films [21]. It is noteworthy that the observed J_{L1} and J_{L2} aggregates are different from the well-known *J* aggregate observed in a homogeneous PIC chloride solution ($\geq\sim$10 mM) at room temperature (we refer this J_S aggregate), which shows a peak energy at $\sim$17 450 cm^{-1} with $\Delta\nu\sim$70 cm^{-1}, and vibronic structures at the higher energy band edge. In a wedge cell made of quartz glass plates, on the other hand, no *J* band was observed at any positions in the cell (6 mM). The results indicate that the J_{L1} and J_{L2} aggregate formation is induced by the surface of the soda lime glass. Since a soda lime glass consists of a lot of exchangeable cations such as Na^+, K^+, and Ca^{2+}, electrostatic interactions between the dye and the anionic sites would facilitate J_L aggregate formation [22]. In a wedge cell made of a borosilicate glass, moreover, the J_{L1} type band with a broad line width (peak: $\sim$17 400 cm^{-1}, $\Delta\nu$: 130 cm^{-1}) was only observed at any position in the cell. The surface of the borosilicate glass also has anionic sites due to borate anions while the amount of dissolvable alkali-metal ions was suppressed to $\sim$20% compared to that for a soda lime glass.[2] The results indicate that the J_{L1} aggregate is produced by adsorption and arrangement of PIC molecules at the anionic sites of the glass surface, while the J_{L2} aggregate is supposed to be grown due to the effects of dissolved alkali-metal ions from the soda lime glass. Since the line width of the J_{L2} band was narrower than that of J_{L1}, it is reasonable to conclude that the size of the J_{L2} aggregate is larger than that of J_{L1} [8]. Indeed, it has been reported that electrostatic interactions are important for *J* aggregate formation in LB films [21]. Spatial distributions of the aggregates in the soda lime glass cell are discussed later in detail.

3.2. Time-resolved fluorescence spectroscopy

Fig. 2 shows fluorescence spectra of the J_{L1} and J_{L2} aggregates observed at the positions of (i) and (ii), respectively. As a characteristic of a *J* aggregate, a Stokes shift is scarcely observed, so that the fluorescence bands of J_{L1} and J_{L2} can be well resolved by varying the observation position in the cell as seen in Fig. 2. Thus, in order to examine exciton dynamics, time-resolved fluorescence measurements were performed. Fig. 3(a) shows fluorescence decays of the J_{L1} and J_{L2} aggregates excited nearly at the absorption peak (570 nm). In order to avoid exciton–exciton annihilation, the excitation intensity was set as low as possible. Under the present conditions, the excited lifetime of a PIC J_S aggregate ($\sim$430 ps) agreed well with the reported value (400 ps) [12]. The fluorescence decay curves of the J_{L1} and J_{L2} aggregates were analyzed by single exponential functions and the emission lifetime of J_{L1} (τ_{L1}=38 ps) determined was faster than that of J_{L2} (τ_{L2}=136 ps). The fluorescence quantum yields of the aggregates at room temperature were estimated roughly to be $\sim$0.03 for J_{L1}

[2]Production catalog of Matsunami Glass Industries.

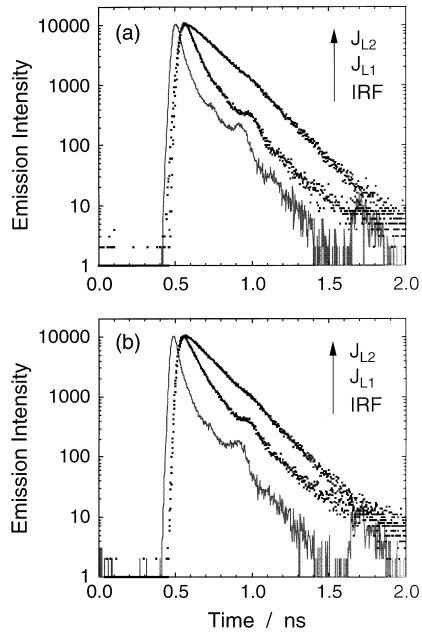

Fig. 3. Fluorescence decay profiles of the J_{L1} and J_{L2} aggregates excited at 570 (a) and 514 nm (b).

and ~0.08 for J_{L2}. Thus, short lifetimes of the J_L aggregates are not due to excitonic superradiance, but to dominant radiationless processes. The fluorescence lifetime of a *J* aggregate adsorbed on solid surfaces is generally shorter than that in a bulk solution [23]. Therefore, the difference in the lifetime between the J_{L1} and J_{L2} aggregates would be ascribed to that in the structures of the PIC aggregates at the glass/solution interface.

An excitation energy dependence of the fluorescence lifetime for the J_L aggregate was examined as the decay profiles of J_{L1} and J_{L2} excited at 514 nm (the tail of the *J* band) were shown in Fig. 3(b). The fluorescence from the monomer was not observed under excitation at 514 nm. By changing the excitation wavelength from 570 to 514 nm (high energy state of the J_L band), τ_{L1} (75 ps) became longer than that at 570 nm excitation while τ_{L2} was almost unchanged (Fig. 3(b)). The results indicate that the J_{L1} aggregate possesses broad size- or structural-distributions. Thus, excitation of the J_{L1} aggregate at a shorter wavelength would lead to larger contributions of the longer lifetime component in the aggregates. On the other hand, the fluorescence lifetime of the J_{L2} aggregate was independent of the excitation wavelength, indicating the fluorescence decay is originated from a single emitting state. The results suggest that the J_{L2} aggregate has narrow size- or structural-distributions. More precisely, the aggregate is made of coherently coupled molecules with a uniform size and structural distribution. The J_{L2} aggregate is suggested to be gradually ordered in accordance with growth of the aggregate. Thus, the self-organized J_{L1} and J_{L2} aggregates have different decay properties owing to the structural differences.

3.3. Total-internal-reflection (TIR) fluorescence spectroscopy

Since absorption and fluorescence lifetime measurements suggested structural and/or morphological differences between the J_{L1} and J_{L2} aggregates, it is worth studying a spatial distribution of the *J* aggregate in the vicinity of the glass/solution interface. Thus, we performed TIR fluorescence spectroscopy. Fig. 4 shows incident angle dependencies of the J_L fluorescence intensities. No change in the spectral band shape was observed for both J_{L1} and J_{L2} aggregates at any incident angles. Since the critical angle (θ_c) for TIR at the soda lime glass/solution interface is ~61°, the data at $\theta_i<\theta_c$ and $\theta_i>\theta_c$ are those under the transmitted and TIR conditions, respectively. The profile was quite different between the J_{L1} and J_{L2} fluorescence. For the J_{L2} aggregate, the fluorescence intensity was almost constant at $\theta_i<\theta_c$ and decreased gradually at $\theta_i>\theta_c$, whereas that for the J_{L1} aggregate increased sharply at $\theta_i<\theta_c$ and decreased very gradually at $\theta_i>\theta_c$. The results indicate that the spatial distribution of the *J* aggregate is different between J_{L1} and J_{L2}, and formation of the J_{L1} aggregate is suggested to be confined to the glass/solution interface. Thus, simulations of the angular profiles in Fig. 4 were performed with Eqs. (1) and (2) as shown by the solid curves. The best fits were attained with $\kappa=1.0\times10^{-3}$ and $h=2$ nm for J_{L1}, and $\kappa=1.5\times10^{-2}$ and $h=300$ nm for J_{L2}. For the J_{L2} aggregate, the simulation reproduced satisfactorily the observed data. In the case of the simulation for the J_{L1} emission, the angle profile was not influenced by a variation of h at ≤2 nm in the region of $\theta_i>\theta_c$, so that h was determined to be 2 nm. However, a discrepancy between the observed and simulated profiles was observed at $\theta_i>\theta_c$ for the J_{L1} aggregate. Furthermore, the J_{L1} concentration estimated from the obtained h and absorbance was considerably higher than that from the obtained κ value. The results indicate that the estimation of h involves some errors for J_{L1} probably due to a rough approximation model in Eq. (2).[3] A possible reason will be an inhomogeneity of the structures and/or distributions of J_{L1} aggregate of PIC. It should be mentioned that the h value is extremely small as compared to the excitation wavelength. However, the TIR emission of a high absorbing sample is now under consideration, so that excitation is expected to confine to the glass/

[3] In the vicinity of a charged surface, an electric double layer is produced toward the solution phase, and the potential normal to the surface is expressed as a Debye–Hückel formula which is an exponential function of z similar to Eq. (2). Since the J_L aggregates is produced by the electrostatic interactions between the glass surface and PIC molecules, the spatial concentration profile of the aggregates (C) in the solution phase is assumed to be expressed approximately by an exponential function of z. Another probable model is a step function; $C=C_0$ at $0\leq z\leq h$ and $C=0$ at $h<z$. In the present case, both models provided quite similar results. Further sophisticated model might fit the observed data for the J_{L1} aggregates. However, the present results show clearly the difference in the spatial distribution of the aggregates between J_{L1} and J_{L2}.

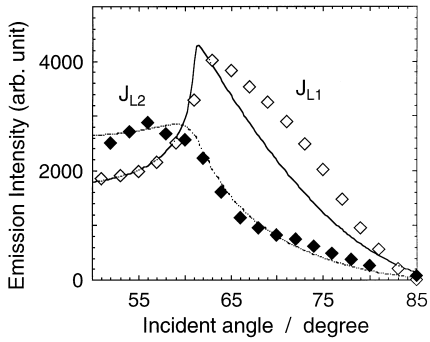

Fig. 4. Incident angle dependencies of the total-internal-reflection (TIR) fluorescence of the J_{L1} and J_{L2} aggregates. The solid curves represent simulated ones on the basis of Eqs. (1) and (2).

solution interface alone, rendering a high resolution for the depth profile. The validity of the h value is now under investigation by atomic force microscope (AFM) measurements [24].

The J_{L1} aggregate is concluded to distribute only in the vicinity of the glass surface with its thickness of $\leq$2 nm. These results indicate that formation of the J_{L1} aggregate is induced by interactions of PIC molecules with the soda lime glass surface and is facilitated by self-organization of the molecules. As a result, the J_{L1} aggregate is produced by adsorption on the glass/solution interface. Such a characteristic is different from that of a J aggregate observed in LB films, where the aggregate is formed in a condensed phase under a pressure. For the J_{L2} fluorescence profile, on the other hand, the simulation of the incident angle dependence of the fluorescence was almost satisfactory. The obtained parameter of h=300 nm indicates that the J_{L2} aggregate formation takes place in a mesoscopic region in the vicinity of the soda lime glass/solution interface. The result indicates that the J aggregate is grown in a soda lime glass wedge cell, as demonstrated by absorption measurements. This h value will be reasonable if the J aggregate possesses a hierarchical structure in size as proposed recently [25]. The relation between the excited decay dynamics and the hierarchical structure of the J aggregate is also a very important problem and worth studying in detail.

3.4. Radiationless channel of the J aggregate at the glass/solution interface

The fluorescence quantum yield and lifetime of the J_{L2} fluorescence were larger than those of J_{L1}, so that the radiationless process should be different between the J_{L1} and J_{L2} aggregates. The h value of the J_{L1} aggregate was smaller than that of the J_{L2}, indicating the interactions between the aggregates and the glass surface are stronger for J_{L1} compared to those for J_{L2}. With decreasing the h value, the contribution of the interactions to the distribution region of the J aggregate in the solution phase increases. Therefore, the radiationless transition rate in the J aggregate interacted strongly with the solid surface is expected to become faster. This is in marked contrast to radiationless transition in the molecular adsorption state, since solute adsorption often suppresses radiationless transitions of the molecule owing to restriction of intra-molecular reorientation and diffusional collision with solvent molecules [26]. An intra-aggregate trap site which induces radiationless processes is proposed as one of the nonradiative channels for J aggregates [27]. Thus, we propose that the interface between the J aggregate and the solid substrate acts as a trap site which dominates the nonradiative channels.

In conclusion, absorption, time-resolved fluorescence, and TIR fluorescence spectroscopies were shown to be a potential means to characterize the structure and optical properties of the J aggregate of the pseudoisocyanine dye. The dye solution in a wedge optical cell consisted of a soda lime glass showed two types of the self-organized J aggregate (J_{L1} for the blue site and J_{L2} for the red site) with different spatial distribution in the solution phase and optical dynamics. The J_{L1} aggregate was confined to the vicinity of the glass/solution interface. The J_{L2} aggregate was suggested to be grown in a mesoscopic region. We expect that time-resolved TIR fluorescence spectroscopy and atomic force microscope measurements will reveal further details about the structure and excited state properties of the J aggregates.

Acknowledgements

The authors thank the reviewer for invaluable comments. They are also indebted to Dr. H.-B. Kim and Mr. Habuchi of this laboratory for their technical assistance in single photon counting measurements. NK is grateful for a grant-in-aid from the Ministry of Education, Science, Sports and Culture (08404051) for partial support of the research.

References

[1] G. Feher, M.Y. Okamura, in: R.K. Clayton, W.F. Sistrom (Eds.), The Photosynthetic Bacteria, Plenum Press, New York, 1978, p. 349.
[2] E. Hanamura, Phys. Rev. B 37 (1988) 1273.
[3] E.E. Jelley, Nature 138 (1936) 1009.
[4] E.E. Jelley, Nature 139 (1937) 631.
[5] G. Scheibe, Angew. Chem. 50 (1937) 212.
[6] F.C. Spano, S. Mukamel, Phys. Rev. A 40 (1989) 5783.
[7] F.C. Spano, J.R. Kuklinski, S. Mukamel, J. Chem. Phys. 94 (1991) 7534.
[8] E.W. Knapp, Chem. Phys. 85 (1984) 73.
[9] H. Fidder, J. Terpstra, D.A. Wiersma, J. Chem. Phys. 94 (1991) 6895.
[10] D.V. Brumbaugh, A.A. Muenter, W. Knox, G. Mourou, B. Wittmershaus, J. Lumin. 31 (1984) 783.
[11] V. Sundström, T. Gillbro, J. Chem. Phys. 83 (1985) 2733.
[12] V. Sundström, T. Gillbro, R.A. Gadonas, A. Piskarskas, J. Chem. Phys. 89 (1988) 2754.
[13] S. De Boer, D.A. Wiersma, Chem. Phys. Lett. 165 (1990) 45.
[14] H.-P. Dorn, A. Müller, Appl. Phys. B 43 (1987) 167.
[15] E. Daltrozzo, G. Scheibe, K. Gschwind, F. Haimerl, Photogr. Sci. Eng. 18 (1974) 441.

[16] T. Karstens, K. Kobs, J. Chem. Phys. 84 (1980) 1871.
[17] R.F. Kubin, A.N. Fletcher, J. Lumin. 27 (1982) 455.
[18] H. Yao, H. Ikeda, N. Kitamura, J. Phys. Chem. B 102 (1998) 7691.
[19] M. Toriumi, M. Yanagimachi, in: H. Masuhara, F.C. DeSchryver, N. Kitamura, N. Tamai (Eds.), Microchemistry; Spectroscopy and Chemistry in Small Domains, North-Holland, Amsterdam, 1994, p. 257.
[20] M. Toriumi, M. Yanagimachi, H. Masuhara, Appl. Opt. 31 (1992) 6376.
[21] R.A. Hall, K. Kajikawa, M. Hara, W. Knoll, Thin Solid Films 295 (1997) 266.
[22] T.M. El-Shamy, Phys. Chem. Glasses 14 (1973) 18.
[23] A.A. Muenter, D.V. Brumbaugh, J. Apolito, L.A. Horn, F.C. Spano, S. Mukamel, J. Phys. Chem. 96 (1992) 2783.
[24] S. Sugiyama, H. Yao, O. Matsuoka, R. Kawabata, N. Kitamura. S. Yamamoto, Chem. Lett. (1999) 37.
[25] K. Misawa, T. Kobayashi, in: T. Kobayashi (Ed.), J-Aggregates, World Scientific, Singapore, 1996, p. 41.
[26] K. Kemnitz, N. Tamai, I. Yamazaki, N. Nakashima, K. Yoshihara, J. Phys. Chem. 90 (1986) 5094.
[27] V.F. Kamalov, I.A. Struganova, T. Tani, K. Yoshihara, Chem. Phys. Lett. 220 (1994) 257.